GSC Advanced Research and Reviews
eISSN: 2582-4597 CODEN (USA): GARRC2
Cross Ref DOI: 10.30574/gscarr
Journal homepage: https://gsconlinepress.com/journals/gscarr/

(RESEARCH ARTICLE)

Growth dynamics and allometric modeling of four commercial forest tree species in Côte d'Ivoire

Anique Ahou Gbotto [1,*], Georges Abéssika Kouakou Yao [1], Beda Innocent Adji [2], Ama Brognan Aimée Kouamé [1], Bi Boh Nestor Goré [1] and Selastique Doffou Akaffou [1]

[1] *Department of Agronomy and Forestry, Genetics Laboratory, University of Jean Lorougnon Guede, BP 150 Daloa, Côte d'Ivoire.*
[2] *University Institute for Timber and Landscape Engineering, University of Jean Lorougnon Guede, BP 150 Daloa, Côte d'Ivoire.*

GSC Advanced Research and Reviews, 2026, 26(01), 079-093

Publication history: Received on 22 June 2025; revised on 04 November 2025; accepted on 06 January 2026

Article DOI: https://doi.org/10.30574/gscarr.2026.26.1.0396

Abstract

Sustainable management and restoration of tropical forests rely on a clear understanding of tree growth dynamics and biomass allocation. In Côte d'Ivoire, extensive forest degradation has drastically reduced the size and diversity of native timber stands, leading to the inclusion of *Terminalia ivorensis* and *Pterygota macrocarpa* on the IUCN Red List. Despite their ecological and commercial importance, the growth patterns and allometric relationships of these species remain poorly documented, limiting the development of reliable models to support forest management and reforestation strategies.

This study aimed to characterize growth and developmental patterns in four commercial species (*Terminalia superba*, *T. ivorensis*, *P. macrocarpa*, and *Mansonia altissima*) cultivated under experimental plantation conditions in Côte d'Ivoire. Growth and biomass allocation were analyzed using the GreenLab functional–structural plant model, based on monitored morphological traits, phyllochron development, and architectural parameters.

The results revealed marked differences among species in leaf emergence rate, internode elongation, and resource allocation. *T. superba* and *T. ivorensis* exhibited faster height and diameter growth, whereas *P. macrocarpa* and *M. altissima* invested proportionally more biomass in foliage. These contrasting patterns reflect distinct adaptive strategies influencing productivity and ecological resilience.

Overall, the study provides new insights into tropical forest tree growth and offers valuable guidance for species selection, modeling, and sustainable reforestation efforts in West Africa.

Keywords: Forest species; Development; Growth; Silviculture; Modeling

1. Introduction

Between 2000 and 2005, several West African countries experienced alarming rates of deforestation. Forest cover declined by approximately 2.5% in Benin, 0.3% in Burkina Faso, 1.0% in Niger, 3.3% in Nigeria, and 4.5% in Togo, while Côte d'Ivoire recorded one of the highest losses in the region, approaching 10% [1–3]. This decline reflects widespread land-use changes driven by agricultural expansion and timber extraction. In Côte d'Ivoire, over 80% of the original forest cover had been lost by the early 2000s, with cocoa cultivation acting as the primary driver [4,5]. Even protected areas were affected, with approximately 38,000 hectares cleared annually between 2001 and 2004 to establish cocoa

* Corresponding author: Anique Ahou Gbotto.

plantations [6]. Between 2000 and 2019, cocoa-driven deforestation and degradation reached 2.4 million hectares, further undermining biodiversity and ecosystem resilience [7].

Forest restoration is therefore a critical environmental priority. Côte d'Ivoire has pledged to restore five million hectares of forest landscapes by 2030 under the Bonn Challenge and promotes agroforestry practices that integrate native tree species while encouraging "zero deforestation" cocoa systems [8,9]. Key commercial timber species include *Terminalia superba*, *T. ivorensis*, *Pterygota macrocarpa*, and *Mansonia altissima*, which are economically valuable but have suffered population decline and reduced genetic diversity. Notably, *T. ivorensis* and *P. macrocarpa* are listed on the IUCN Red List of Threatened Species [10].

Reforestation efforts using species such as *T. ivorensis*, *T. superba*, and *Tectona grandis* have faced setbacks due to high mortality within a decade [11]. Developing resilient plant varieties through genetic selection is a promising strategy to improve reforestation success [12]. Additionally, architectural modeling provides insights into growth dynamics and biomass allocation, supporting silvicultural practices tailored to ecological and economic objectives. Although such modeling has been applied to species like *Eucalyptus* [13], *Tectona grandis* [14], *Khaya senegalensis* and *Parkia biglobosa* [15], and *Pterocarpus erinaceus* [16], no studies have yet examined the architectural growth of key commercial timber species in Côte d'Ivoire.

This study therefore aims to characterize growth dynamics and biomass allocation in four major timber species using functional–structural modeling. By elucidating species-specific growth patterns, the research seeks to inform sustainable reforestation strategies and improve forest management in Côte d'Ivoire.

2. Materials and methods

2.1. Experimental site

The experiment was conducted from September to December 2018 in the central-western region of Côte d'Ivoire, located between latitudes 4°30′N and 10°30′N, and longitudes 2°30′W and 8°30′W. The study site is situated 21 km from the town of Daloa, at coordinates 6°39′1″N and 6°30′48″W. The region experiences a tropical climate characterized by four distinct seasons: a long rainy season (April to mid-July), a short dry season (mid-July to mid-September), a short rainy season (mid-September to November), and a long dry season (December to March). The average annual rainfall is approximately 1200 mm. During the study period, temperatures ranged from 24.65°C to 27.75°C, and the mean relative humidity was around 95%.

2.2. Plant material, treatments, and experimental design

Eleven, six-month-old seedlings from each of the four species under study: *Terminalia superba* (Fraké), *Terminalia ivorensis* (Framiré), *Pterygota macrocarpa* (Koto), and *Mansonia altissima* (Bété) were selected as the experimental material. For clarity, these species will hereafter be referred to by their local names, as indicated in parentheses. All seedlings were propagated from seed. Figure 1 illustrates the juvenile stages of the respective species.

Figure 1 Young plants of *Terminalia ivorensis* (A), *Terminalia superba* (B), *Pterygota macrocarpa* (C), and *Mansonia altissima* (D)

Fifteen two-month-old seedlings were planted in five rows per species, with both intra-row and inter-plant spacing set at 30 cm. A 50 cm gap was maintained between species. Seedlings were watered daily throughout the experiment. Insect

infestations were managed using Decis® Bayer insecticide, applied at a concentration of 8 mL per 16 L of tap water. Weeding was carried out manually as needed.

To monitor the dynamics of organ development and growth (leaves and internodes), measurements were taken at two-week intervals on five individuals per species. These measurements focused on the length and diameter of the internodes, as well as the length and width of the leaves. The measurements began with the first internode from the base, since the stem was actively growing and new leaves were emerging. The observations were conducted over a two-month period (from October to December 2018). Diameters were measured using a caliper, while lengths and widths were taken using a 30 cm graduated ruler.

2.2.1. Field data collection and structural encoding

In the field, measurements were first recorded on data sheets and subsequently transcribed into the Multiscale Tree Graph (MTG) format [17] using Microsoft Excel. This methodology facilitates a comprehensive understanding of plant structure and is applicable to a wide range of plant species. The structural composition of forest species is described through three primary types of topological relationships:

Decomposition relationships, such as the breakdown of an axis into phytomers;

- Succession relationships, referring to the sequential formation of two entities by the same apical meristem (e.g., the emergence of two consecutive metamers);
- Filiation relationships, in which a daughter entity arises from a parent entity through branching (e.g., a lateral branch emerging from the main stem).

These relationships collectively define the topology of the plant [17], which is read from the collar (plant base) to the apex. The plant's topological structure is encoded using a formal syntax based on the aforementioned relational rules.

In this study, the plant architecture was described using the following hierarchical components: individual (N), axis (A), internode (e), and leaf (f). Each component, or vertex, is assigned an index that denotes its branching order (from 1 to 3), distinguishes between alternate leaves, or indicates the node rank from base to apex. A symbol preceding the vertex denotes the nature of the topological relationship: "<" indicates a succession relationship, "+" indicates a filiation relationship, "/" indicates a decomposition relationship. The encoded sequence is read from left to right, and the symbol "^" is used to indicate a relationship with a vertex located above, in the same column of the spreadsheet. Measured variables were associated with specific structural units, such as the internodes (e1, e2, e3…) and leaves (f1, f2). All collected architectural data were compiled into an MTG file, which summarizes the complete dataset used for structural analysis. The data were extracted from the MTG format using Xplo software, integrated within the AMAPstudio platform [18].

2.2.2. Study of biomass and allometric relationships

For this study, six individuals from each species were fully harvested and dissected (Figure 2). The position of each phytomer along the axis was recorded by assigning a rank from the apex downward, allowing accurate spatial referencing within the bearing axis. Measurements focused on both internodes (Figure 2A) and leaves (Figure 2B) along the main axis (A1, corresponding to the trunk) and secondary branches (A2 and A3).

Figure 2 Internodes (A) and leaves (B) dissected for the biomass study

For each leaf, the following parameters were recorded: blade length and width, petiole length, leaf area, and fresh and dry mass. Leaf blade length (Lf) was measured along the central vein using a ruler. Leaf width (lf) was recorded at the midpoint of the blade, perpendicular to the central vein. Leaf area (Sf) was determined by scanning each leaf using an HP G4010 scanner, followed by digital analysis with the Leaver Education module, an extension of the Toaster plugin. Toaster (Tree and planT Organs and Structures Analyzer) is an open-source ImageJ plugin developed by CIRAD [19]. It includes several modules for analyzing biological structures, with the Education module specifically designed for academic use. Measurements taken on internodes included length (Len), measured directly with a ruler; diameter (Den), measured at the midpoint (½ of total length) using a caliper; volume (Ven), estimated by modeling the internode as a cylinder, using the formula:

$Ven=\pi r^2 h$, where $r=\frac{1}{2}Den$ and h = Len (the length of the internode).

Dry mass of both leaves and internodes was determined after oven-drying at 70°C for 72 hours, followed by weighing on a precision balance with an accuracy of 0.001 g.

2.3. Development traits tested

- The morphological parameters analyzed included: plant height, stem diameter, number of internodes, leaf dimensions, and growth rate.
- Height was measured from the collar to the apex, and diameter was measured at the collar.
- The number of internodes was counted from the first internode following the cotyledonary leaves up to the apex.
- Leaf dimensions were measured as previously described.
- The growth rate was calculated over a two-month period as the difference between the final and initial diameter, divided by 60 days.

2.3.1. Phyllochron

The phyllochron refers to the time interval between the successive emergence of phytomers. It was calculated by dividing the total number of phytomers produced by the trunk over an eight-month period by the number of days (240). The species-specific phyllochron corresponds to the average value calculated across individuals of the same species. This approach aligns with current methods used to assess thermal and temporal regulation of leaf appearance [20].

2.3.2. Time of functioning and expansion

Functioning time (Tf) and expansion time (Ta) were calculated based on data extracted from the MTG file. The functioning time (Tf) of the organs corresponds to the lifespan of the leaves, specifically the period during which they actively perform photosynthesis. Functional leaves are green, in contrast to non-functional (senescent) leaves, which are yellow. Tf was determined by counting the number of nodes bearing green leaves along the main stem. This count was then converted into developmental cycles. The expansion time (Ta) refers to the duration required for a leaf to reach its final, maximum size.

2.4. Statistical analysis

A descriptive analysis of the data was performed to calculate dispersion parameters, including the minimum and maximum values, mean, and standard deviation of the morphological traits across species. Next, a one-way analysis of variance (ANOVA) was conducted to compare the species. This was followed by a Newman–Keuls post hoc test at a defined significance level to enable pairwise comparisons. Finally, a principal component analysis (PCA) was performed to assess the structuring of morphological diversity within each species. Allometric relationships were evaluated using linear regression. All analyses were conducted using Statistica software, version 7.1 [21].

3. Results

3.1. Plants and species variability

Descriptive analysis revealed significant variability in the measured parameters, both within species and between species. For Koto, the collar diameter of the seedlings had an average of 0.69 ± 0.05 cm, ranging from 0.61 to 0.81 cm (Table 1). The mean height was 28.45 ± 5.06 cm, with values ranging from 18.00 to 35.10 cm. The number of internodes also showed notable variation, with an average of 10.82 ± 0.87, ranging from 10 to 13. Similar variability was observed in growth rate, as well as leaf length and width. In the case of Bété, the collar diameter averaged 0.76 ± 0.08 cm, with a

range of 0.59 to 0.90 cm (Table 1). The mean height was 38.56 ± 9.31 cm, varying from 21.20 to 48.70 cm. The number of internodes also varied significantly, with an average of 16.55 ± 2.42, ranging from 12 to 20. These trends were consistent for growth rate and leaf dimensions (length and width). For Fraké, the measured seedlings had a mean collar diameter of 1.05 ± 0.18 cm, ranging from 0.70 to 1.35 cm (Table 1). The mean height was 92.21 ± 15.90 cm, with values ranging from 60.10 to 115.10 cm. The number of internodes averaged 39 ± 6.65, with a range of 28 to 47. Once again, similar patterns of variation were observed for the growth rate and leaf size parameters.

For Framiré, variations were also observed in the collar diameter among the measured seedlings, with a mean value of 1.05 ± 0.18 cm (Table 1), ranging from 0.80 to 1.33 cm. Similar variability was noted in plant height, which averaged 103.58 ± 8.66 cm, with values ranging from 81.60 to 115.57 cm. The number of internodes also showed variation, with a mean of 41.73 ± 2.97, ranging from 39 to 49. These differences were likewise observed for other variables such as growth rate, leaf length, and leaf width. Overall, comparison across the four species indicates that the most vigorous seedlings were found in Framiré and Fraké (Table 1).

Table 1 Mean values of seven morphological traits measured across four species, with minimum and maximum values shown in brackets

Variables	Koto	Bété	Fraké	Framiré
Dc	0.69 ± 0.05^{a} (0.61 – 0.81)	0.76 ± 0.08^{a} (0.59-0.90)	1.05 ± 0.24^{b} (0.70-1.35)	1.05 ± 0.18^{b} (0.8-1.33)
Hm	28.45 ± 5.06^{a} (18-35.10)	38.56 ± 9.31^{a} (21.20-48.70)	92.21 ± 15.90^{c} (60.10-115.10)	103.58 ± 8.66^{d} (81.60-115.57)
Nen	10.82 ± 0.87^{c} (10-13)	16.55 ± 2.42^{b} (12-20)	39 ± 6.65^{a} (28-47)	41.73 ± 2.97^{a} (39-49)
Len	2.64 ± 0.50^{a} (1.8-3.51)	2.33 ± 0.42^{a} (1.41-2.74)	2.37 ± 0.24^{a} (22.83)	2.51 ± 0.24^{a} (1.94-2.76)
Vc	0.28 ± 0.03^{a} (0.23-0.34)	0.22 ± 0.07^{a} (0.11-0.38)	0.42 ± 0.16^{b} (0.18-0.66)	0.50 ± 0.17^{b} (0.32-0.89)
Lf	25 ± 3.42^{b} (21.36-30.72)	23.93 ± 2.82^{ab} (18.38-29.49)	24.06 ± 3.33^{ab} (17.96-28.79)	21.47 ± 1.71^{a} (19.50-24.34)
lf	11.94±2.78^{b} (9.17-17)	11.63 ± 1.04^{b} (9.30-13.14)	7.73 ± 0.88^{a} (6.70-8.88)	6.50 ± 0.52^{a} (5.81-7.22)

For each traits, values with the same letters within a row are statistically similar; Dc: collar diameter (cm); Hm: mean trunk height (cm); Nen: number of internodes; Len: internode length (cm); Vc: growth rate (cm); Lf: leaf length (cm); lf: leaf width (cm).

3.2. Organization and structuring of plant and species variability

The principal component analysis (PCA) results revealed three main factors. The first factor (PC1) accounted for 58.35% of the total variability and is loaded with collar diameter (Dc), mean height (Hm), number of internodes (Nen), growth rate (Vc), and leaf width (lf) (Table 2). This axis represents a vigor-related factor, with all four variables positively correlated with factor 1. The second factor (PC2), defined by leaf length, represents variation in leaf size and explains 22.95% of the total variability (Table 2). The third factor (PC3) is associated with internode length and corresponds to a structural or architectural factor, explaining 12.40% of the total variability. Plotting the species on a two-dimensional plane reveals two distinct groups (Figure 3). The first group (G1) includes Fraké and Framiré, characterized by larger collar diameters, greater heights, more internodes, and higher growth rates. However, these species have smaller leaves. In contrast, the second group (G2) includes Koto and Bété, which display smaller collar diameters, shorter heights, fewer internodes, and lower growth rates, but possess larger leaves. Notably, intraspecific variability is also observed, indicating a degree of diversity among individuals within species.

Table 2 Eigenvectors, eigenvalues and inertia percentage explained by the three first canonical variables for seven traits analyzed in four species

Eigenvector	PC1	PC2	PC3
Eigenvalue	4.08	1.61	0.87
Inertia percentage	58.35	22.95	12.4
Cumulative inertia percentage	58.35	81.3	93.7
Traits			
Dc	0.88*	0.33	-0.22
Hm	0.96*	0.06	0.17
Nen	0.97*	-0.02	-0.01
Len	-0.09	0.59	0.8*
Vc	0.82*	0.39	-0.12
Lf	-0.25	0.88*	-0.31
lf	0.83*	0.46	-0.17

Dc: collar diameter; Hm: mean trunk height; Nen: number of internodes; Len: internode length; Vc: growth rate; Lf: leaf length; lf: leaf width.
*Significant value: variables that contribute the most to axe formation

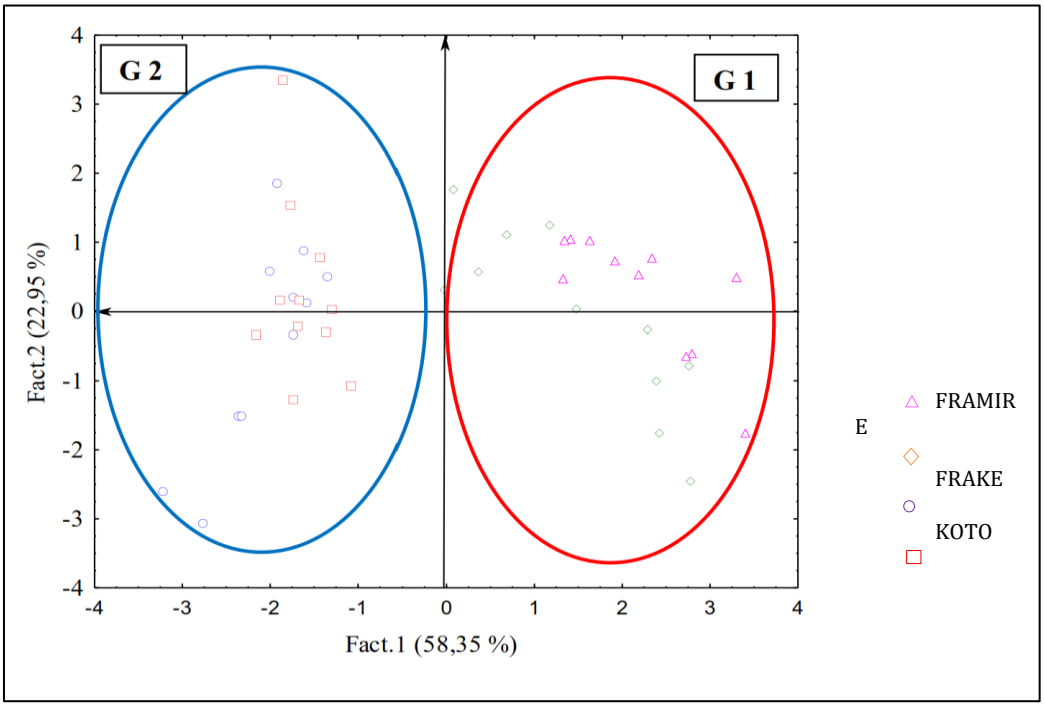

Fact. 1: factor 1; Fact. 2: factor 2; G1: group 1; G2: group 2

Figure 3 Plotting the species on a two-dimensional plane revealed by the PCA according to the type of factor

3.3. Development parameters of the GreenLab model

3.3.1. Phyllochron

The calculated phyllochron was 5 days for Framiré and 6 days for Fraké (Table 3). For Bété and Koto, the phyllochron was 14 and 23 days, respectively. Comparisons indicate that Framiré and Fraké do not differ significantly from each other, but both contrast with Bété and Koto, which also differ from one another.

Table 3 Timing of phytomer emission in the four species

Axes / Species	Phyllochron				
	A1	A2	A3	A4	A
Fraké	7 ± 1.44	6 ± 0.86			6.36 ± 1.26
Framiré	5.94 ± 0.22	4.29 ± 1.90	5.31 ± 1.94	6.33 ± 2.99	4.99 ± 2.10
Koto	23.13 ± 1.19	-	-	-	23.13 ± 1.19
Bété	14.71 ± 1.21	-	-	-	14.71 ± 1.21

3.3.2. Study of leaf expansion duration

Figure 4 shows leaf expansion over time. As illustrated, the leaves of Framiré, Fraké, and Bété reached their final size after 28 days, while in Koto, full expansion was achieved after 42 days. These time points thus define the expansion duration of the respective organs.

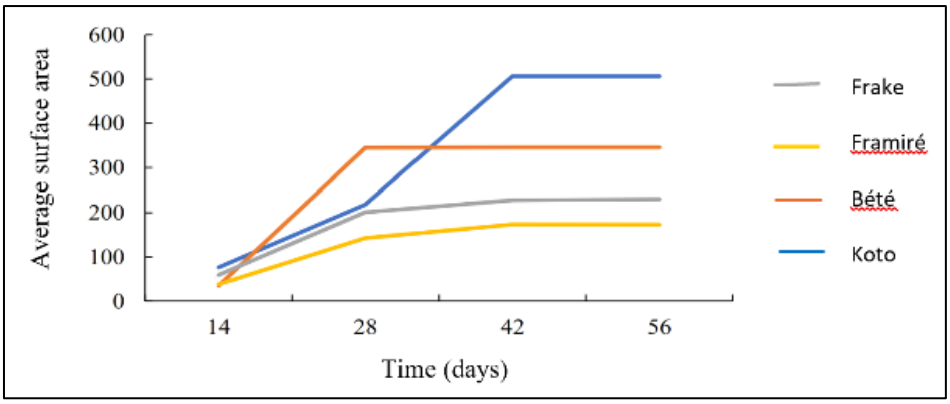

Figure 4 Leaf expansion duration across species

3.3.3. Study of functional duration

The calculated functional duration was 29 CD for both *Framiré* and *Fraké*. In contrast, for *Koto* and *Bété*, the functional duration was 10 and 13 CD, respectively. These values indicate that *Framiré* and *Fraké* are similar, whereas *Koto* and *Bété* are more closely related to each other.

3.4. Growth analysis

Linear regressions between the dimensions of fresh organs and their dry mass were used to establish allometric equations specific to each species. Subsequently, a general equation was selected to estimate the dry mass of the various organs across the four species.

3.4.1. Study of Koto growth

Linear regressions revealed a near-perfect correlation between dry biomass and internode volume (Figure 5a), described by the allometric equation y = 0.44 × volume. For leaves, dry biomass correlated strongly with the product of length and width (Figure 5b), yielding y = 0.004 × (length × width). Theoretical biomass estimates derived from these equations showed excellent agreement with measured values ($R^2 \geq 0.95$; Figures 6 a, b), underscoring their predictive accuracy.

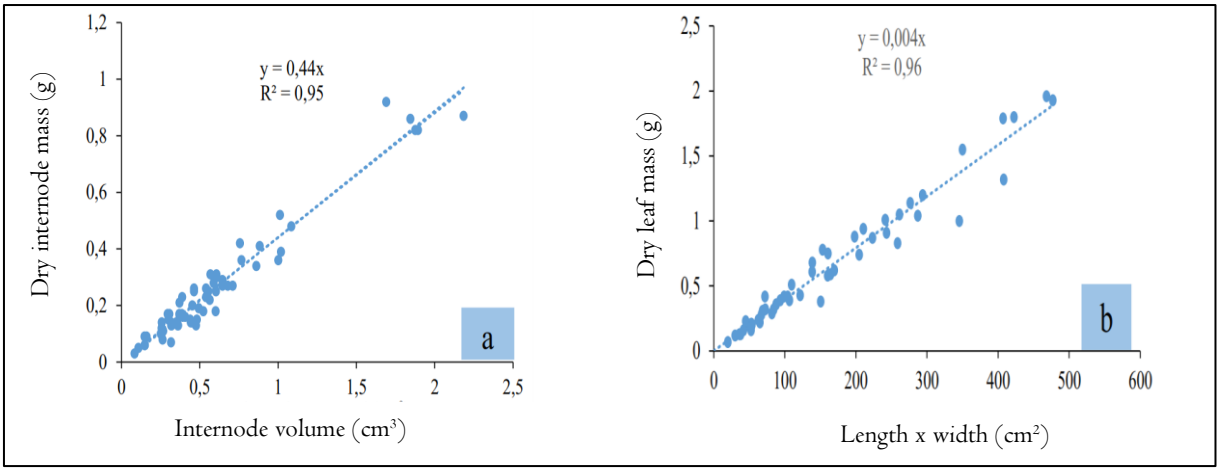

Figure 5 Linear regression: (a) between dry internode mass and its volume, and (b) between dry leaf mass and the product of its length and width in Koto

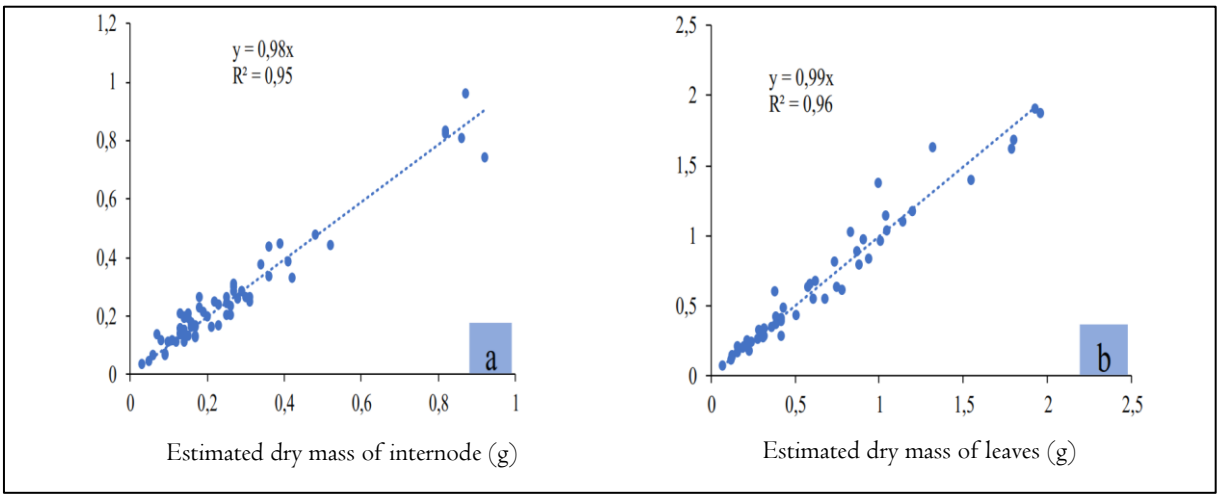

Figure 6 Relationship between observed and estimated dry biomass (a) of internodes and (b) of leaves in Koto

3.4.2. Study of Bété growth

In Bété, the derived linear regressions revealed a strong correlation ($R^2 > 0.9$) between dry biomass and internode volume (Figure 7a), described by the allometric equation y = 0.39 × volume. For leaves, dry biomass was strongly correlated with the product of leaf length and width (Figure 7b), with the relationship expressed as y = 0.003 × (length × width). Predicted dry biomass values obtained from these equations were also highly correlated with the observed data ($R^2 > 0.9$), confirming the robustness of the models (Figures 8a and 8b).

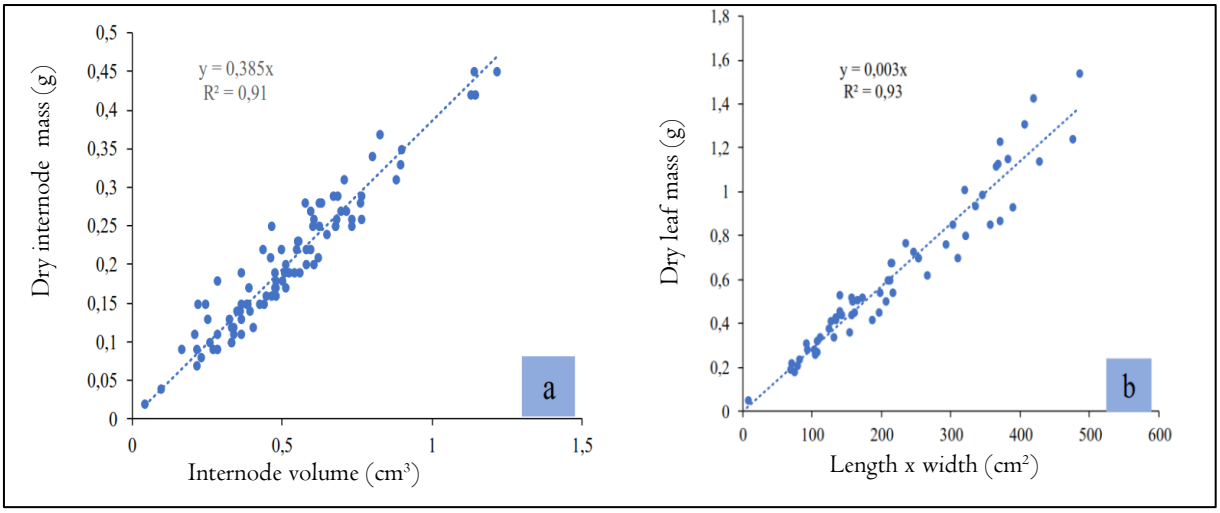

Figure 7 Linear regression: (a) between dry internode mass and its volume, and (b) between dry leaf mass and the product of its length and width in Bété

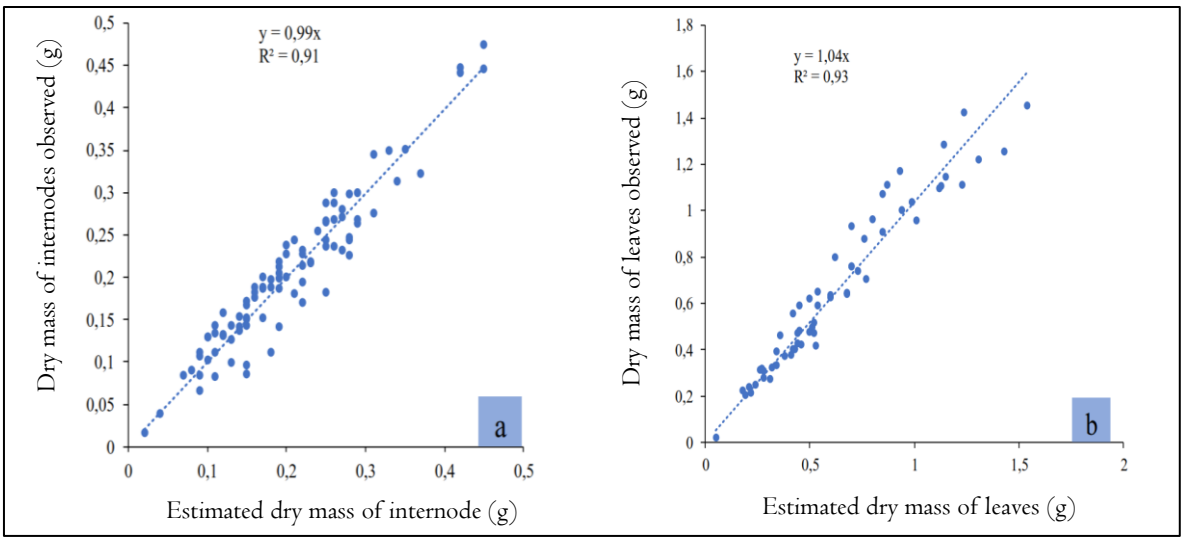

Figure 8 Relationship between observed and estimated dry biomass (a) of internodes and (b) of leaves in Bété

3.4.3. Study of Fraké growth

In Fraké, the linear regression results revealed a strong relationship ($R^2 > 0.8$) between dry biomass and internode volume (Figure 9a). The relationship was described by the equation: y = 0.34 × volume. A similar trend was observed for leaves (Figure 9b), with the relationship expressed as: y = 0.002 × (length × width). Theoretical biomass values calculated using these equations also exhibited a high degree of correlation ($R^2 > 0.8$), as shown in Figures 10a and 10b.

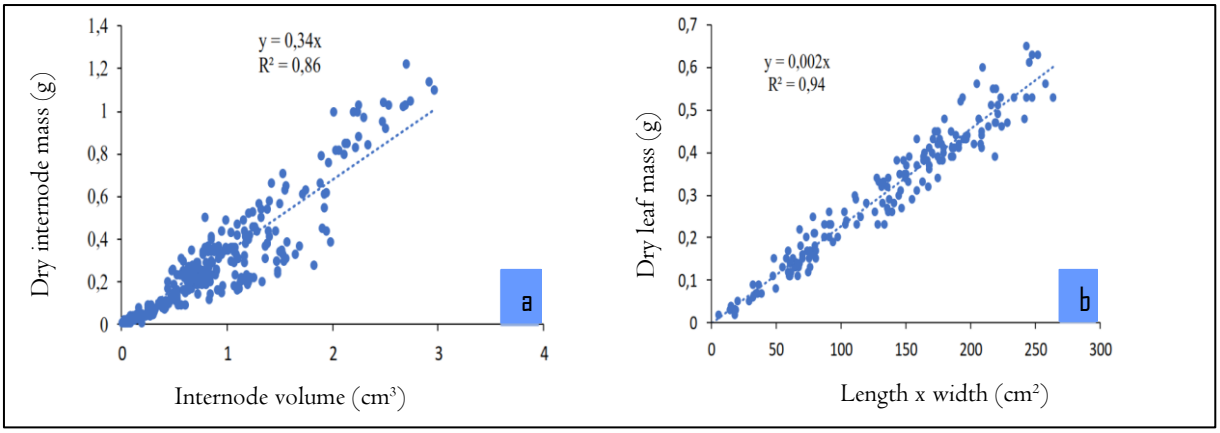

Figure 9 Linear regression: (a) between dry internode mass and its volume, and (b) between dry leaf mass and the product of its length and width in Fraké

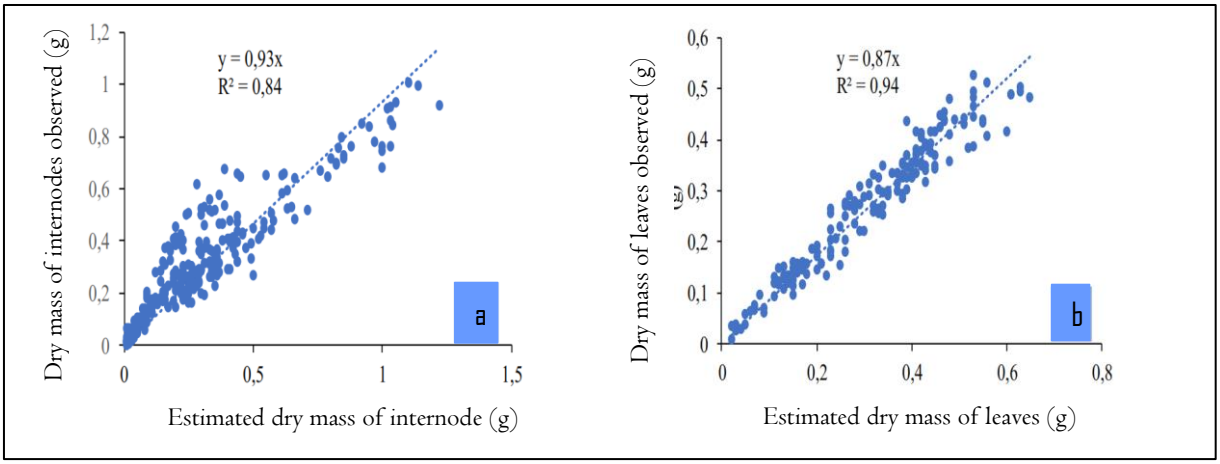

Figure 10 Relationship between observed and estimated dry biomass (a) of internodes and (b) of leaves in Fraké

3.4.4. Study of Framiré growth

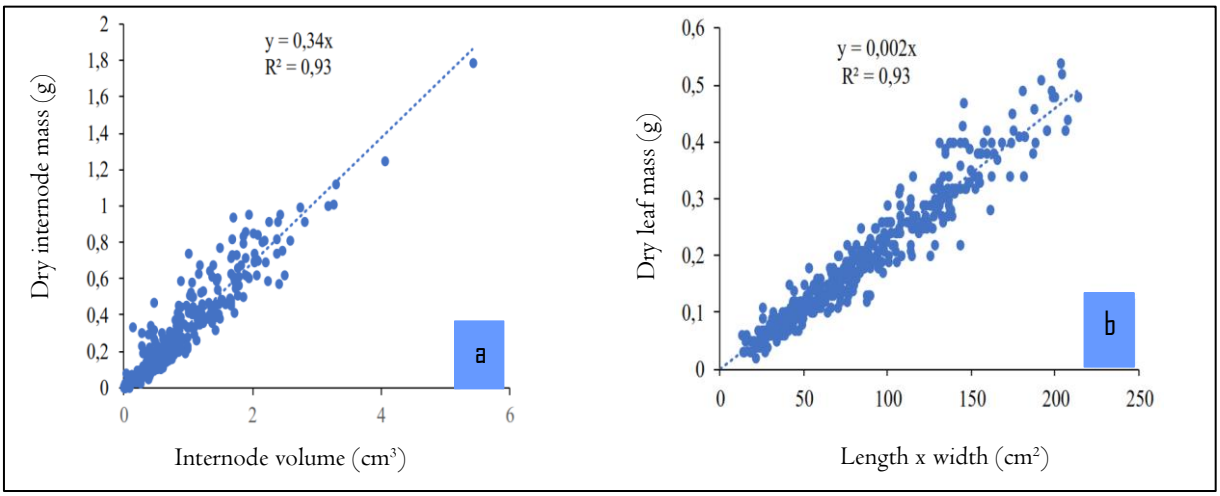

Figure 11 Linear regression: (a) between dry internode mass and its volume, and (b) between dry leaf mass and the product of its length and width in Framiré

Finally, in *Framiré*, the linear regression analysis revealed a strong correlation (R^2 > 0.93) between dry biomass and internode volume (Figure 11a), described by the equation: y = 0.34 × volume. A similarly strong relationship was observed for leaves (Figure 11b), expressed as: y = 0.002 × (length × width). Theoretical biomass values calculated from these equations also showed a high correlation (R^2 = 0.93), as illustrated in Figures 12a and 12b.

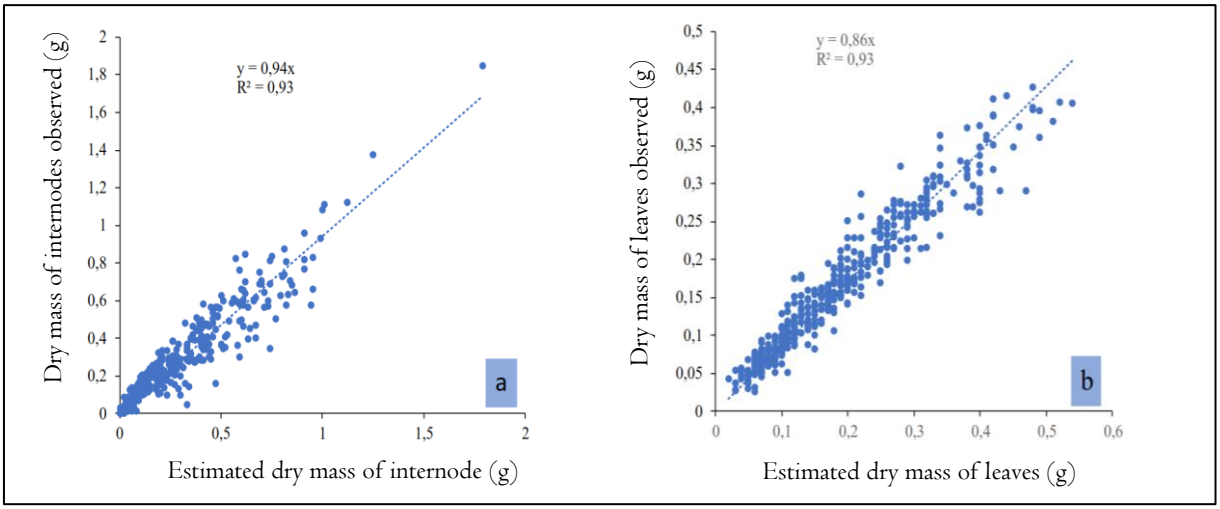

Figure 12 Relationship between observed and estimated dry biomass (a) of internodes and (b) of leaves in Framiré

3.4.5. Generalization of allometric equations for four species

Linear regressions across all species (Koto, Bété, Fraké, Framiré) showed a strong correlation ($R^2 \geq 0.9$) between observed and estimated dry biomass of internodes and leaves (Fig. 13a, b).

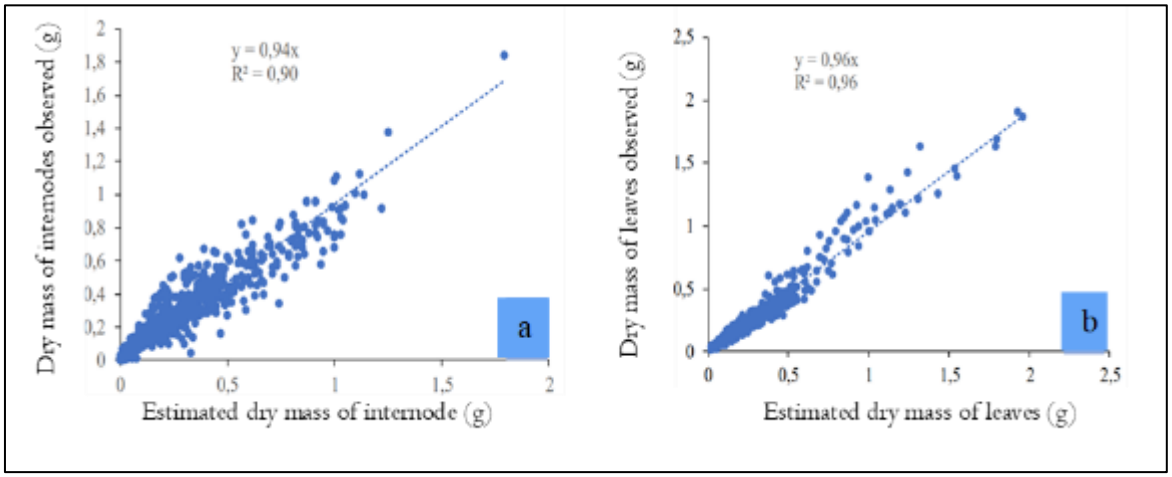

Figure 13 Relationship between observed and estimated dry biomass (a) of internodes and (b) of leaves in Koto, Bété, Fraké, and Framiré

4. Discussion

This study investigated growth and developmental parameters in four forest species. The findings revealed significant variation both among species and within species. While interspecific variation was expected, intraspecific differences may be attributed to the reproductive system, namely allogamy, which, as noted by Barrett [22], enhances intraspecific diversity.

Among the species studied, Framiré (*Terminalia ivorensis*) and Fraké (*Terminalia superba*) exhibited the greatest vigor, with markedly higher growth rates than Koto (*Pterygota macrocarpa*) and Bété (*Mansonia altissima*). These results suggest that Framiré and Fraké are particularly suitable candidates for reforestation programs.

Phyllochron analysis further highlighted interspecific differences. Bété and Koto displayed longer phyllochrons (15 and 23 days, respectively), consistent with their lower vigor and slower growth rates. Conversely, Framiré and Fraké

showed shorter phyllochrons, a greater number of internodes, and smaller leaves, reflecting a higher allocation of resources to the production of new organs rather than to organ expansion.
Comparable findings have been reported in coffee species. Soualiou [23] and Okoma [24] observed phyllochron variation in relation to species, habitat, and climate, with internode emission times in *Coffea canephora* reaching up to 30 days, similar to the value recorded here for Koto (23 days). By contrast, the 15-day phyllochron reported by De Reffye et al. [25] closely aligns with the value obtained for Bété.

Leaf longevity proved to be a central determinant of photosynthetic capacity and overall growth strategy across the four studied species. Species with longer leaf functioning time (Fraké, Framiré: ~29 CD) exhibited higher leaf number and thus maintained higher potential photosynthetic surface area compared to Koto and Bété (~10–13 CD). These findings align with recent evidence that variation in leaf lifespan is strongly associated with phenological traits such as leaf production periods and reproductive investment in a range of woody and herbaceous taxa [26]. Moreover, among evergreen tree species, studies indicate that though photosynthetic capacity per leaf mass declines with age, the integrated CO_2 assimilation over the entire lifespan of leaves may not scale up with increased longevity, due to diminishing returns from older leaves. Mediavilla & Escudero [27] & Niinemets *et al.* [28], recently showed similar patterns. Ecologically, shorter leaf lifespan has also been found to be adaptive under stress: for example, in conifers from the Northern Hemisphere, species with shorter leaf longevity recovered more rapidly from drought-induced damage and suffered less mortality during hot, dry summers than species with long-lived foliage [29]. Thus, our results suggest that while longer leaf duration contributes to cumulative carbon fixation via increased photo-active leaf area, trade-offs in maintenance costs and declining photosynthetic efficiency with leaf age may modulate the net benefit, especially under environmental stress.

The expansion period measured for *Framiré*, *Fraké*, and *Bété* revealed close similarity among these three species, while *Koto* differed significantly. This divergence likely reflects differing survival or growth strategies, as suggested by Adji et al. [30]. Regarding biomass, no comparable study has yet been conducted for the forest species *Koto*, *Bété*, *Fraké*, and *Framiré* in Côte d'Ivoire. Biomass and its partitioning among woody plant components are known to be influenced by many factors including plant architecture, morphology, plant age, and climatic variables [31]. In our work, we derived robust allometric equations linking dry mass to fresh-organ dimensions in all species. Specifically, for internodes we obtained an equation $y=0.38\times volume$, and for leaves $y=0.003\times(length\times width)$, both with coefficients of determination $R^2\geq0.90$. These equations allow reliable estimation of dry masses of internodes and leaves in the studied species.

Comparable allometric relationships have been reported recently for other tropical and subtropical species. For example, Zhao *et al.* [32] examined 151 tree species across China and observed strong, species-specific allometries linking stem, leaf, and root biomass, and showed that life-history traits strongly modulate allometric coefficients. Similarly, the recent study [33] found that leaf area scales isometrically with the metabolically active sapwood volume across height growth in *Ricinus communis*, underscoring the importance of organ morphology in predicting biomass allocation.

In this study, the strongest correlation with total biomass was found for leaf biomass ($R^2=0.96$). With stem (or internode) biomass showing slightly lower but still high predictive power ($R^2=0.90$). Overall, leaves are superior predictors of biomass compared to stems in these species. These are the first allometric equations produced for *Koto*, *Bété*, *Fraké*, and *Framiré*. Moreover, recent work under elevated CO_2 regimes (e.g. Loblolly pine studies) has shown that allometric relationships themselves may shift under changing environmental conditions, altering biomass allocation in predictable ways [34, 35]. Thus, while our equations serve as a strong baseline for biomass estimation in these species, they may need adjustment if environmental conditions (CO_2 concentration, climate) differ substantially from those under which the data were gathered.

The allometric models reported for coffee internodes by [24] achieved exceptionally high goodness-of-fit ($R^2=0.99\%$); nevertheless, the leaf–biomass correlations reported in that work are closely comparable to those obtained in the present study.

This outcome may be attributed to a conducive environment as well as the influence of genotypic variation among individuals [24]. All the equations obtained were validated by a strong correlation between the observed and estimated data. Similar high-quality fits have been reported for other woody and cultivated species, including forest trees such as teak (*Tectona grandis*) [36], and cultivated plants such as cotton (*Gossypium hirsutum*) [25], sunflower (*Helianthus annuus*) [37], maize (*Zea mays*) [38], and wheat (*Triticum aestivum*) [39], six Malagasy coffee species [23]. Although performance can vary with species, sample structure, and environment [40]. In West African contexts, recent multispecies allometric studies and inventory analyses [41] confirm that locally derived, species- or site-specific models outperform generic pantropical equations and often yield very high R^2 values when calibrated on well-sampled populations (see regional allometry syntheses and dry-forest inventories). The high correspondence between observed

and predicted values across our equations demonstrates that organ-level allometries (internodes, leaves) reliably predict dry mass in these species, a pattern also observed for Coffea and other woody taxa. For example, non-destructive allometries relating stem volume to stem dry mass and leaf area to leaf dry mass have proven robust in African *Coffea* species [24].

Nonetheless, lower predictive power has been reported in some coffee studies [40], where R^2 values fell to ~0.80 or less; the authors attributed such reductions to variation in plant age, sampled size range, and climatic variability, factors that also likely influence the models presented here. Finally, species-level reports for *Terminalia spp*. and for *Mansonia altissima* (Bété) indicate that timber-tree allometries and biomass accumulation patterns are strongly site- and species-dependent, reinforcing the need for locally parameterized equations such as those produced in this study [42].

5. Conclusion

This study provides a detailed characterization of growth and developmental patterns in four major forest species—Koto, Bété, Fraké, and Framiré. The results show substantial variation in morphological traits both within and among species. Koto and Bété exhibit similar growth behavior, while Fraké and Framiré display faster growth and greater overall vigor. The analysis also reveals marked species-specific differences in phyllochron, expansion time, and functioning time. Fraké and Framiré present the shortest phyllochron and the longest functioning period, whereas Koto and Bété show slower leaf emergence and shorter functioning duration. In addition, this work establishes a reliable allometric method to estimate dry mass from fresh organ dimensions, providing a practical tool for future biomass assessments.

Although the objectives of the study were achieved, further work is needed to strengthen and extend these findings. Increasing the sample size to 30 individuals per species would improve result accuracy, while crown architecture analysis would provide deeper insights into branching patterns and developmental probabilities. Growth modeling would also help identify production surfaces and sink strengths. Finally, expanding the study to other threatened species, such as Mahogany and Tiama, would support broader conservation and reforestation strategies.

Compliance with ethical standards

Disclosure of conflict of interest

No conflict of interest to be disclosed. All authors confirm that they have no financial, personal, or institutional relationships that could be perceived as influencing the work reported in this manuscript.

References

[1] Horning N. Remote sensing analysis of tropical forest change. In: *Tropical Forestry Handbook*. 2nd ed. Berlin: Springer; 2018. p. 1–25.

[2] Geist HJ, Lambin EF. Proximate causes and underlying driving forces of tropical deforestation. *Bioscience*. 2002; 52(2): 143–50.

[3] Pouliot M, Pyakurel U, Smith-Hall C. Forest use practices and deforestation: case studies from West Africa. *For Policy Econ*. 2012; 18: 48–56.

[4] Lunku HS, Li Z, Yang S, Shayo A, Ngoma JB, Ngoma J. The dynamics of deforestation in sub-Saharan Africa: the impact of environmental policy and foreign direct investment on forest conversion. *For Policy Econ*. 2024; 169: 103342.

[5] Wingate V, Grogan K, Anderson W. Drivers of cocoa-related deforestation across West Africa. *Land Use Policy*. 2024; 133: 106961.

[6] McNicol I, Ryan CM, Mitchard ETA. Carbon losses from deforestation and degradation in tropical agricultural frontiers. *Glob Change Biol*. 2018; 24(11): 4861–74.

[7] Pendrill F, Gardner TA, Meyfroidt P, Persson UM, Adams J, Azevedo T, Lima MGB, Baumann M, Curtis PG, De Sy V, Garrett R, Godar J, Goldman ED, Hansen MC, Heilmayr R, Herold M, Kuemmerle T, Lathuillière MJ, Ribeiro V, Tyukavina A, Weisse MJ, West C. Disentangling the numbers behind agriculture-driven tropical deforestation. Science. 2022; 377(6611): eabm9267.

[8] Renier C, Vandromme M, Meyfroidt P, Ribeiro V, Kalischek N, zu Ermgassen EKHJ. Transparency, traceability and deforestation in the Ivorian cocoa supply chain. Environ Res Lett. 2023; 18(2): 024030.

[9] Carodenuto S. Cocoa sector governance for zero deforestation cocoa in Côte d'Ivoire. *Sustainability*. 2019; 11(7): 1697.

[10] IUCN. *IUCN Red List of Threatened Species*. Version 2009. Gland: IUCN; 2009.

[11] Mitchual SJ. Survival and growth performance of indigenous and exotic species in reforestation trials in West Africa. *J For Res*. 2014; 25(4): 853–8.

[12] Boulier F, Collin P. Genetic improvement in tropical timber species: progress and prospects. *Ann For Sci*. 2009; 66(7): 702.

[13] Diao J, De Reffye P, Lei X, Guo H, Letort V. Simulation du développement topologique de jeunes Eucalyptus à l'aide d'un modèle stochastique et d'une stratégie de mesure d'échantillonnage. Comput Electron Agric. 2012; 80: 105–114.

[14] Tondjo K, Brancheriau L, Sabatier SA, Kokutse AD, Akossou A, Kouami KK, Jaeger M, de Reffye P, Fourcaud T. Architectural development of *Tectona grandis*: a model-based study. *Trees*. 2015; 29: 1215–28.

[15] Adji BI, Akaffou DS, Letort V, Kang MZ, Wang X, Jaeger M, De Reffye P, Kouassi KH, Duminil J, Cilas C, Sabatier S. Functional–structural modeling of *Khaya senegalensis* and *Parkia biglobosa*. *Agrofor Syst*. 2022; 96: 133–48.

[16] Adji A, Mbow C, Gning O. Growth architecture and biomass allocation in *Pterocarpus erinaceus*. *Trees*. 2022; 36: 395–409.

[17] Pradal C, Godin C. MTG as a standard representation of plants in FSPMs. In: Kahlen K, Chen TW, Fricke A, Stützel H, editors. Book of abstracts of the 9th International Conference on Functional–Structural Plant Models (FSPM 2020); 2020 Oct 5–9; Hannover, Germany. Hannover: Institute of Horticultural Production Systems; 2020. p. 86–87.

[18] Griffon S, de Coligny F. AMAPstudio: an integrated platform for plant architecture modeling. *Ann Bot*. 2014; 114(4): 813–26.

[19] CIRAD. Leaver Education module (Toaster plug-in for ImageJ). Montpellier: CIRAD; 2010.

[20] Parent B, Tardieu F. Temperature responses of developmental processes. *New Phytol*. 2012; 194(3): 760–774.

[21] StatSoft Inc. *Statistica* (version 7.1). Tulsa, OK: StatSoft; 2005.

[22] Barrett SCH. Understanding plant reproductive diversity. *Philos Trans R Soc B*. 2010; 365: 99–109.

[23] Soualiou S, Wang Z, Sun W, de Reffye P, Collins B, Louarn G, Song Y. Functional–structural plant models in crop science. *Front Plant Sci*. 2021; 12: 747142.

[24] Okoma P, Akaffou S, De Reffye P, Hamon P, Hamon S, Konan O, Kouassi KH, Legnate H, Letort V, Sabatier S. Estimation of stem and leaf dry biomass using a non-destructive method applied to African Coffea species. Agrofor Syst. 2018; 92(3): 1–9.

[25] de Reffye P., Blaise F., Chemouny S., Jaffuel S., Fourcaud T. and Houllier F. (1999). Calibration of a hydraulic architecture-based growth model of cotton plants. Agronomie, 19 (3-4) 265-280.

[26] Li FL, Liu X, Bao WK. Leaf lifespan and phenology relationships. Ecol Evol. 2016; 6: 3822–3831.

[27] Mediavilla S, Escudero A. Photosynthetic capacity over leaf lifetime. New Phytol. 2003; 159(1): 203–211.

[28] Niinemets Ü, Uwe K, Peter H, Staudt M, Arneth A, Cescatti A, Ciccioli P, Copolovici L, Geron C, Guenther AB, Kesselmeier J, Lerdau MT, Monson RK, Penuelas J. Estimations of isoprenoid emission capacity. *Biogeosciences*. 2011; 8: 2209–2246.

[29] Sterck FJ, Song Y, Poorter L. Drought- and heat-induced mortality of conifers. *Sci Adv*. 2024; 10(15): eadl4800.

[30] Adji BI, Letort V, Wang X, Kang, M., De Reffye, P, Jaeger, M, Cilas, C, Kouassi, K H, Duminil, J, Sabatier, S, & Akaffou, D S. Rethinking iconic species reforestation in West Africa. *Forests*. 2023; 14(7): 1311.

[31] Guo Z, Fang J, Pan Y, Birdsey R. Estimates of forest biomass carbon stocks. *For Ecol Manage*. 2010; 259(7): 1225–1231.

[32] Zhao M, Tian S, Zhu Y, Li Z, Zeng S, Liu S. Allometric relationships across tree species. *Ecosphere*. 2021; 12(5): e03522.

[33] Berry E, Anfodillo T, Castorena M, Echeverría A, Olson ME. Scaling of leaf area with biomass. *J Exp Bot*. 2024; 75(13): 3993–4004.

[34] Gao X, Koven CD, Kueppers LM. Allometric trade-offs in grasses. *Ecol Appl*. 2024; 34(4): e2976.

[35] Kim D, Medvigy D, Maier CA, Johnsen K, Palmroth S. Biomass increases under elevated CO_2. *Glob Change Biol*. 2020; 26(4): 2519–2533.

[36] Tondjo K, Brancheriau L, Sabatier SA, Kokutse AD, Akossou A, Kouami KK, Fourcaud T. La variabilité des propriétés clés du bois est-elle liée à la variabilité des caractéristiques architecturales clés ? Cas du teck planté au Togo selon l'éclaircissage et la provenance. Ann For Sci. 2015; 72: 717–729.

[37] Rauf S, Shahzad M, da Silva JAT, Noorka IR. Biomass partitioning in sunflower. *J Crop Sci Biotechnol*. 2012; 15: 53–57.

[38] Guo, Y, Ma, Y, Zhan, Z, Li, B, Dingkuhn, M, Luquet, D, & de Reffye, P. Optimization of the GreenLab model for maize. *Ann Bot*. 2006; 97(2): 217–230.

[39] Kang MZ, Cournède PH, de Reffye P, Auclair D, Hu BG. Analytical study of a stochastic growth model. *Math Comput Simul*. 2008; 78(1): 57–75.

[40] Negash M, Starr M, Kanninen M, Berhe L. Allometric equations for *Coffea arabica*. *Agrofor Syst*. 2013; 87: 1451.

[41] Gueulou N, Coulibaly B, Fayolle A, Ouattara DN, Ahoba AK, N'guessan A, Bakayoko A. Tree allometry in dryland forests of Côte d'Ivoire. *Trees For People*. 2024; 15: 100478.

[42] De Ridder M. Tree-ring analysis and stem biomass estimation of limba (*Terminalia superba* Engl. & Diels) in the framework of sustainable forest management [PhD thesis]. Ghent, Belgium: Ghent University, Faculty of Bioscience Engineering; 2013.